LAWRENCE
LIVERMORE
NATIONAL
LABORATORY

UCRL-JRNL-214218

Nonlinearly Additive Forces in Multivalent Ligand Binding to a Single Protein Revealed with Force Spectroscopy

T. V. Ratto, R. E. Rudd, K. C. Langry, R. L. Balhorn, M. W. McElfresh

August 1, 2005

Langmuir

Nonlinearly Additive Forces in Multivalent Ligand Binding to a Single Protein Revealed with Force Spectroscopy

Timothy V. Ratto[*,1], *Robert E. Rudd*[2], *Kevin C. Langry*[1], *Rodney L. Balhorn*[3], *Michael W. McElfresh*[1].

1- Chemistry and Materials Science, Lawrence Livermore National Laboratory, L-232, 7000 East Ave. Livermore, CA 94550

2- Physics and Advanced Technologies, Lawrence Livermore National Laboratory, L-045, 7000 East Ave. Livermore, CA 94550

3- Biology and Biotechnology Research Program, Lawrence Livermore National Laboratory, L-452, 7000 East Ave. Livermore, CA 94550

AUTHOR EMAIL ADDRESS: ratto7@llnl.gov

RECEIVED DATE

TITLE RUNNING HEAD: Multivalency Measured with Force Spectroscopy

ABSTRACT: We present evidence of multivalent interactions between a single protein molecule and multiple carbohydrates at a pH where the protein can bind four ligands. The evidence is based not only on measurements of the force required to rupture the bonds formed between ConcanavalinA (ConA) and α-D-mannose, but also on an analysis of the polymer-extension force curves to infer the polymer architecture that binds the protein to the cantilever and the ligands to the substrate. We find that

although the rupture forces for multiple carbohydrate connections to a single protein are larger than the rupture force for a single connection, they do not scale additively with increasing number. Specifically, the most common rupture forces are approximately 46, 66, and 85 pN, which we argue corresponds to 1, 2, and 3 ligands being pulled simultaneously from a single protein as corroborated by an analysis of the linkage architecture. As in our previous work polymer tethers allow us to discriminate between specific and non-specific binding. We analyze the binding configuration (i.e. serial versus parallel connections) through fitting the polymer stretching data with modified Worm-Like Chain (WLC) models that predict how the effective stiffness of the tethers is affected by multiple connections. This analysis establishes that the forces we measure are due to single proteins interacting with multiple ligands, the first force spectroscopy study that establishes single-molecule multivalent binding unambiguously.

KEYWORDS force spectroscopy, multivalent, protein-carbohydrate, single-molecule, polymer, tethers

INTRODUCTION

The role of protein-carbohydrate interactions in biological systems has attracted a great deal of attention in recent years. These interactions are now known to mediate cell-cell recognition including the infection of cells by bacteria and viruses, to play a variety of roles in the regulation of enzymes and other proteins, and to be directly involved in cancer progression and metastasis.[2-4] In addition, the recognition and binding of carbohydrates is involved in the cellular transport of glycoproteins,[5] and the apical targeting of membrane proteins.[6] One intriguing detail in protein-carbohydrate interactions is that affinities between single carbohydrate ligands and proteins are quite weak.[7,8] As most lectins (carbohydrate-binding proteins) are found as oligomeric rather than monomeric molecular species, this suggests Nature has overcome the weak carbohydrate-binding problem by utilizing multivalent interactions, where binding strength is enhanced through multiple simultaneous connections. Because of this enhancement, researchers have attempted to make multivalent high affinity ligands synthetically with the proposed future goal of producing high-affinity inhibitors of carbohydrate-mediated pathogenic adhesion.[9-12] There has been significant progress in this area, with many groups reporting molecules with equilibrium affinities that are three orders of magnitude greater than the affinities of the individual ligands and show promising inhibitory properties toward toxins, bacteria, and viruses. Despite this success it has been difficult to ascribe a specific molecular interpretation to the enhancement effect. Firstly, many analyses of protein-carbohydrate multivalency utilize agglutination assays to measure the enhancement in affinity rather than adhesion. Recent findings indicate that these assays measure cross-linking and aggregation rather than reversible binding and consequently may not be relevant to the design of multivalent inhibitors.[13,14] Secondly, bonds between adhesion molecules often undergo mechanical stresses leading to conformational changes in the proteins. These changes can have large effects on binding properties (force transduction)[15-17] and few assays have the ability to characterize the bonds mechanically. Finally, all binding affinity measurements are by their nature ensemble measurements that measure many thousands (or millions) of interactions simultaneously. Ensemble

measurements tend to produce averaged values wherein the range of energies is blurred together into a single value, which may obscure important non-equilibrium aspects of the interaction.

Force spectroscopy techniques; such as optical tweezers, AFM, and biomembrane force probes, offer the potential to overcome the above complications and produce data that may clarify the mechanisms behind multivalency.[16,17] These methods- involving moving two functionalized surfaces together and measuring the force required to pull the surfaces apart- have the potential to measure single protein-ligand bond rupture forces and determine how applied forces affect bond strength. Although some of the first published force spectroscopy measurements were made on multivalent protein-receptor systems,[18,19] these early seminal force measurements suffered from two significant shortcomings. Firstly, the binding proteins were attached directly to the AFM cantilever rather than though polymer tethers, making it difficult to separate specific from nonspecific interactions. Secondly, and more importantly, the authors made no effort to restrict the number of proteins on their AFM cantilever. Instead they performed the experiments in the presence of excess protein in the buffer solutions and relied on the excess protein to block the majority of interactions. Although blocking with protein certainly would reduce the number of binding events between the tip and the substrate, it does not guarantee that the measurements consist of single protein-receptor events as we present here.

We report on our measurements and analysis of the forces involved in rupturing multiple ligand connections to single proteins, which we believe to be the first time single-protein multivalency has been demonstrated in a force spectroscopy experiment. As in our previous studies of monovalent binding[1] we investigate the interaction between polymer-tethered ConcanavalinA (ConA) proteins and similarly tethered mannose ligands to determine the forces required to rupture the protein-ligand bonds, as well as ascertain the specific effects on binding due to the presence of the tethers. As we and others have shown,[1,20,21] the polymer tethers allow the specific interactions to be spatially discriminated from the non-specific. Also as we have shown previously, by only taking data with functionalized cantilevers that show single interactions at tip-sample separation distances that approximate two polymer lengths, the tethers permit a validation of single protein interactions. We choose our tip-functionalization

chemistry specifically to limit the number of active proteins on the cantilever. Although there may be other proteins attached to the tip, they do not participate in the specific binding force curves due to the tip curvature, or other physical or chemical constraints that prevent the formation of specific bonds with the molecules on the functionalized surface. Fitting a subset of the force curves with modified polymer chain models allows us to determine if the polymer connection due to protein-ligand bonding between the tip and substrate behaves as two polymers connected in series (essentially a single PEG tether with one protein-carbohydrate bond), as two polymers connected in parallel (essentially a single tether with twice the stiffness and two protein-bonds bonds), or as a branched configuration (one protein bound to multiple carbohydrates.) We use a standard worm-like chain (WLC) model as a starting point for our analysis of the polymer stretching as the WLC model has been shown to accurately capture the mechanical behavior for polymer chains.[22-25]

Previously we controlled our system to guarantee no multiple interactions. Here we vary the pH and investigate the effect of the pH-dependent valency of ConA. This protein exists as a tetramer at biological pH (~7.4), as do many other carbohydrate-binding proteins or *lectins*, but disassociates to dimers at lower pH's,[1,20,21] thus serving as an ideal system to investigate multivalency. These highly accurate measurements offer the possibility of developing an understanding of the molecular mechanisms behind the increased adhesion forces due to multivalent interactions.

EXPERIMENTAL

Tip Functionalization. A process similar to that described previously[1] was used to functionalize AFM cantilevers with PEG-tethered ConA, except that here a higher pH was used. Briefly, silicon nitride cantilevers were silanized from the vapor phase using recently distilled 3-aminopropyltriethoxysilane (APTES) and methyltriethoxysilane (MTES) at an amino to methyl ratio of 1/250 to reduce the number of active groups on the tip. Di-functional polyethylene glycol (PEG) tethers were then used to attach the ConcanavalinA protein to the AFM cantilever. The MTES is therefore used to dilute the APTES, and the controlling factor in the functionalization is thus not the PEG or ConA concentrations but rather the ratio of the methylsilane to the aminosilane molecules we use to attach the

PEG to the tip. We use a high concentration of PEG (10 mg/ml) in order to prevent the di-NHS functional PEG's from "bridging" or linking between two aminosilanes on the tip. The final step is to attach the protein to the other end of the tether through amino groups (lysines) in the protein.

Substrate Functionalization. A process similar to that described earlier [1] was used to functionalize the substrate with PEG-tethered mannose. Briefly, self-assembled monolayers (SAMs) were formed on gold-coated silicon by immersing the substrates in 1 mM 16-mercaptohexadecanoic acid. After rinsing in ethanol and chloroform, polymer tethers were attached to the SAMs and functionalized with α-D-mannopyranosylphenyl isothiocyanate to generate a substrate that displayed mannose carbohydrates linked to the substrate through polymer tethers. The polymer tethers displayed molecular weights between 2614 and 3893 amu (corresponding to between 20-30 nm in extended length) as measured by MALDI.[1]

All points of attachment between the protein and the tip and the ligand and the substrate consist of covalent bonds. At bond loading rates comparable to the rates we use in this study, covalent attachments have bond rupture forces in excess of 1000 pN,[26] thus we can be confident that the rupture forces we measure are not due to the polymer tethers being removed from either the tip or the substrate.

Finally, in order to guarantee that our cantilevers are functionalized with low numbers of polymer-tethered proteins, we discard tips that display multiple interactions at greater than single tether lengths (> 29 nm) with frequencies higher than 0.5%. We have examined each of the remaining double-rupture events and did not find any case that appeared to be caused by two specific bond ruptures; i.e. that displayed the characteristic polymer extension and bond rupture force associated with specific binding. Usually, one rupture appeared to be specific while the other rupture was caused by a rare nonspecific interaction extending out from the substrate in a series of ruptures. This down selection and validation of the tips essentially guarantees that the measured events at double-tether lengths from the substrate are due to single-molecule interactions.

Force Spectroscopy. A Nanoscope IIIa (Digital Instruments, Veeco, Santa Barbara, CA) was used to control a commercial Bioscope AFM in force calibration mode. Deflection vs. Z-piezo travel

measurements were performed at 1 Hz and at amplitudes of 120 nm. As previously discussed[1] we used a 5-10 nm trigger to control tip-substrate contact area and upon triggering delayed the retraction of the cantilever for 1 second to allow time for the protein to find and bind the ligands. All measurements were carried out in pH 7.4 phosphate buffered saline. The spring constants of the standard Si_3N_4 cantilevers (Veeco, Santa Barbara, CA) were calibrated using the thermal noise method in fluid.[27-29]

Data Analysis. Cantilever deflection vs. z-piezo distance curves were analyzed using Igor Pro (WaveMetrics, Inc. Lake Oswego, Oregon) and a collection of macros written for Igor Pro by Dmitri Venezov, modified here to facilitate bond rupture detection. Prior to analysis the deflection values are converted to force by multiplying by the experimentally determined spring constant[30] and rescaled in x from z-piezo distance to actual tip-sample separation by removing the deflection of the lever. As many curves show optical interference due to spill-over of the laser from the cantilever[30] these effects are subtracted from the force curve in the form of a sine function where the natural frequency of the diode laser is fixed but the phase and amplitude of the interference is allowed to vary. The resulting straight line for deflection of the lever far from the surface is then used to determine the zero of force.

Igor Pro (WaveMetrics, Inc. Lake Oswego, Oregon) was also used to fit the modified WLC models to the force traces utilizing the Levenberg-Marquardt algorithm to minimize the chi-squared value. Since the data contains noise that obscures the local values for the curve and makes it difficult to assess the error associated with model fits to the data, we used a Padé approximated[31] model-independent fit to the data to generate a smooth line through each force trace. The model fits are compared to the Padé approximant by taking the absolute value of the distance between each point in the model fit and each point in the Padé approximant. The average of these values is reported as average error in the text.

RESULTS AND DISCUSSION

In this section we analyze the results of the experiments and present evidence of multivalent interactions between a single protein molecule and multiple carbohydrates at the higher pH where the protein is a tetramer. The evidence for multivalency is based on measurements of the force required to

rupture the bonds formed between ConA and α-D-mannose, on an analysis of the forces on the polymer architecture that binds the protein to the cantilever and the ligands to the substrate, and on an examination of the characteristic tip-sample separation distances at which the polymer-tethered bonds rupture. The section is organized as follows. First blocking experiments are presented in order to identify those events in the force curves associated with the rupture of specific binding of the protein to the carbohydrate. Next rupture-extension distributions are compared at the two values of pH to search for the effect of the transition from dimeric to tetrameric ConA. We then present the distribution of rupture forces at the higher pH. Next we turn to an analysis of the forces due to the extension of the polymers just prior to the specific bond rupture, including a comparison to the force-extension laws for various polymer architectures. We conclude this section with a discussion of the rupture location distributions.

In our earlier work[1] we used AFM direct force measurements to measure both the strength of the adhesive interactions between the polymer-tethered ConA protein and the mannose functionalized substrate, and the tip-sample separation distance at which the interactions took place. A plot of the frequency of adhesive interactions versus tip-sample separation distance shows clusters of interactions that could be roughly correlated with single and double tether lengths. Blocking the interaction by adding unbound mannose to the buffer solution revealed that the clusters at roughly twice the tether length contained the specific ConA-mannose bond rupture interaction. Figure 1A (without blocking) and 1B (with the specific interaction blocked) show our previously published results for the monovalent interaction taken at a pH of 6.0, where ConA is found as a dimer. The specific binding peak is clearly present only in the unblocked experiment. As discussed in the earlier paper, although ConA possesses two binding sites at this pH we suspect that the attachment of the polymer to the protein sterically prevents binding to one of the sites leading to monovalent interactions.

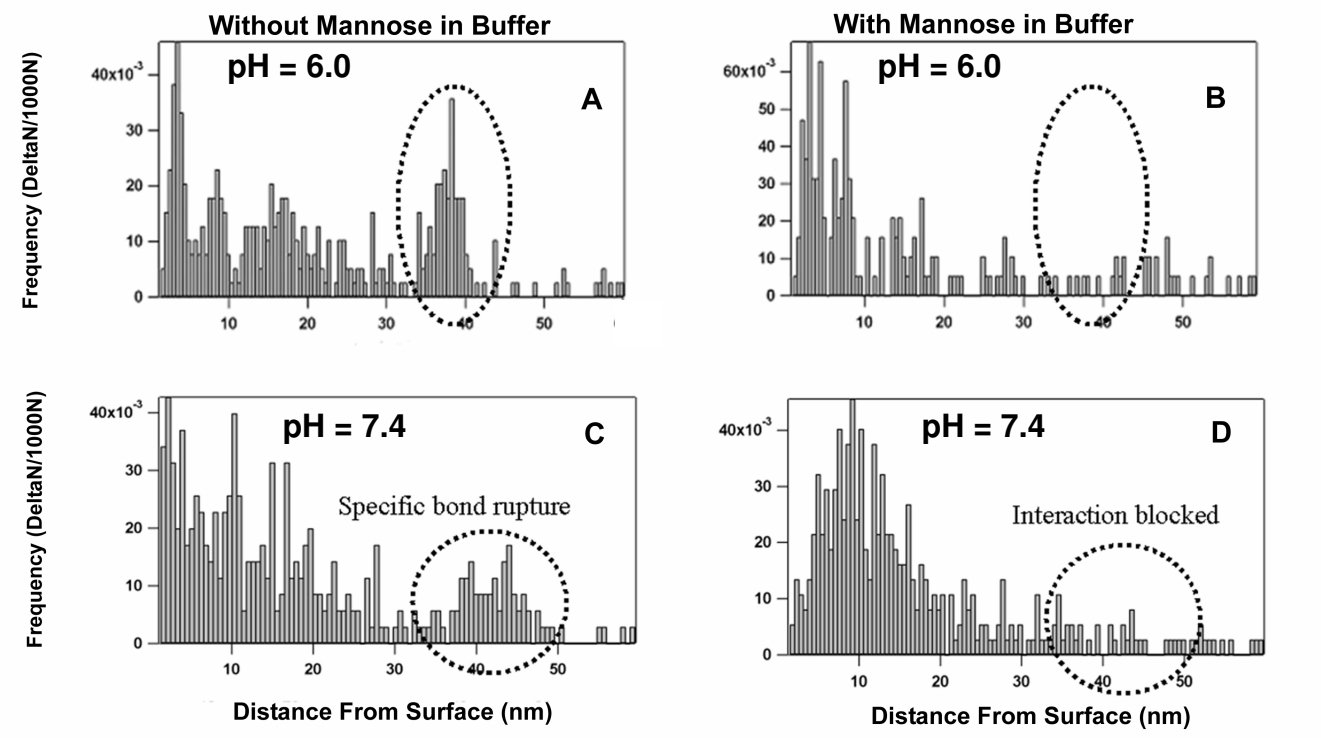

Figure 1. Histograms of the interaction frequency at increasing distances from the point of contact between an AFM tip and a mannose-functionalized surface for data taken at pH 6.0 (1A and 1B reprinted with permission from the Biophysical Journal) and at pH 7.4. Note that at the higher pH ConA takes the form of a tetramer or higher order conjugate. The circled clusters in 1A and 1C show the specific interactions between the ConA and mannose. When the buffer solution in the AFM liquid cell is exchanged with buffer containing free mannose, binding between the ConA on the AFM tip and the mannose attached to the substrate is blocked, and the specific interactions decrease (1B and 1D.) The multiple peaks seen within the circled region in 1C offer evidence for multivalency as discussed below.

We should point out that in order for us to correctly interpret our tip-sample separation distance histograms; only data taken with a single tip are used to produce these histograms. If data from different tips are combined, the peaks in the distance histograms become smeared out due to differences in the location of the polymer-tethered protein on the AFM tip for different tips (the polymer can be anywhere along the radius of curvature of the tip), as well as the variations in the length of the attached polymer.

Unfortunately this requirement greatly limits the amount of data that can be used to produce each distance histogram as each tip can only be touched to a substrate between ~500-3000 times (translating into ~50-300 specific interactions) before it no longer produces reliable data. Force histograms (e.g. Fig. 2) do not suffer from this limitation however, as the spring constant for each cantilever is determined independently, allowing the data from multiple cantilevers to be normalized and combined.

As ConA is found as a tetramer at biological pH rather than a dimer, we were curious as to whether there was a measurable difference in the force required to rupture the protein-ligand bond at higher pHs in comparison to our earlier experiments performed at lower pHs. We postulated that as the tetrameric protein could potentially bind additional ligands, the measured force required to rupture the protein-carbohydrate bond should be higher. We present the evidence for this increase in strength below. First we address the question of whether the measured jumps in the force-distance curves are associated with specific ConA-mannose bond rupture. As in our previous work, we found interactions clustered in distance with the final cluster being approximately two polymer tether lengths away from the point of tip-sample contact (Fig. 1C), as expected when the ConA-mannose bond ruptures takes place at the end of fully extended PEG tethers.

Measured Forces. In our effort to understand how additional binding sites on a protein affect the bond rupture forces, we evaluated the specific interaction cluster from the tip-sample separation histogram and graphed the interactions as a function of frequency versus force (Fig. 4.) The force distribution displayed multiple peaks indicating multiple distributions of forces. The first peak was located at approximately 46 pN, corresponding to the previously measured monovalent bond rupture force, while the second and third most common forces measured were ~66 pN and ~85 pN. This nonlinear increase in force is a somewhat surprising result, as previous force spectroscopy studies have indicated that bond rupture forces are linearly additive with increasing numbers of interactions. For example, the interaction between biotin and streptavidin has been measured as ~160 pN, 320 pN, and 460 pN, with 160 pN being assigned as the monovalent bond rupture force, and the increasing quantized forces being attributed to divalent and trivalent interactions.[18]

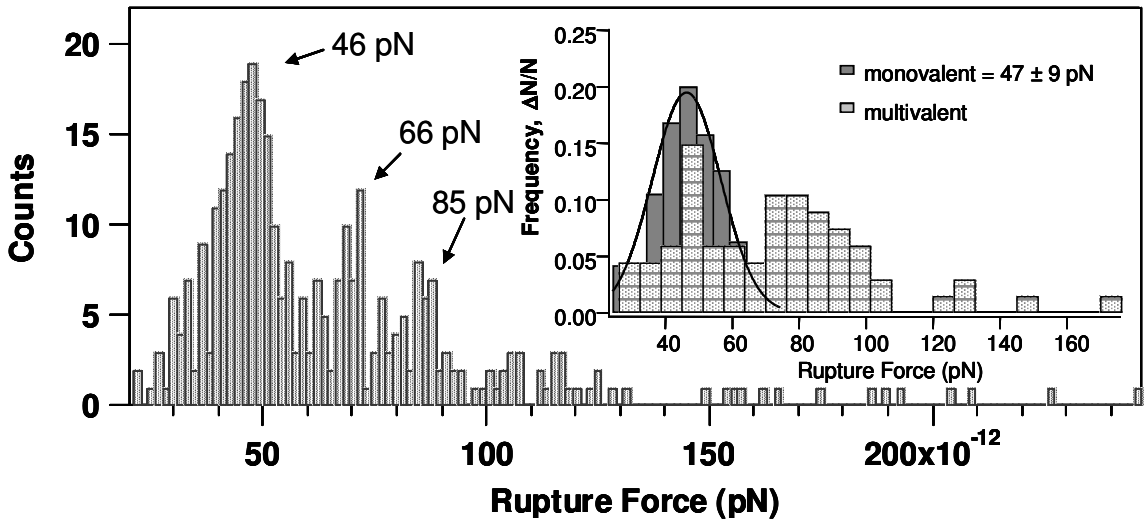

Figure 2. Histograms of the rupture force frequencies for 423 specific interactions measured with 5 different tips at a pH where ConA is found as a tetramer. Three peaks in the histogram are clearly evident; ~46 pN (corresponding to our monovalent measurement from an earlier study), 66 pN, and 85 pN. The inset figure shows two data sets taken from single tips: dark grey shows the force distribution at a pH where ConA is found as a dimer (based on our earlier study[1] we believe that the attachment of the polymer tether to the protein interferes with one of the binding sites on the protein resulting in monovalent binding); light grey is data taken at a pH where ConA is found as a tetramer or higher order aggregate. Because the number of data points that can be obtained using a single tip is small, the two multivalent peaks at 66 pN and 85 pN in the force histogram are not resolved but rather blurred together into a single peak at approximately 80 pN. When data from multiple tips are combined, three peaks are clearly defined.

At first glance this linear additivity appears reasonable; if one bond is strong then two should be twice as strong and so on. However, as others have postulated[32-34] this inference is not correct for all cases. A better (more general) model of the rupture of a single bond takes into account that it is a thermally activated process. Consider the case of the cantilever and the substrate held together by multiple attachments. If the bonds have identical barrier energies, are wholly cooperative, and disassociate simultaneously, the attachment will act as a single bond with the rupture force given by the sum of the individual rupture forces. Under most conditions this scenario is an improbable combination of events,

however, as it is unlikely for the bonds to rupture at exactly the same moment or to be at the identical positions within their energy landscapes. As pointed out in the literature, differences in the load distribution together with the thermally activated, nonlinear rupture laws favor rupture when one bond carries more of the load, and consequently the rupture force scales sub-linearly with bond number. Linearity is expected in cases of identical bonding, such as with multiple protein-ligand pairs and when the mean force is large compared to the width of the rupture force distribution, as was the case in the earlier experiments.

Several theories have been proposed for the rupture of multiple and multivalent bonds. One simple theory is that the applied force loads all of the N bonds equally and that all of the bonds are identical and rupture at a well-defined force. Furthermore, it might be assumed that once one bond ruptures, the increased load on the remaining bonds causes them to rupture immediately. Then the relationship between the rupture force of N bonds, f_N, to that of a single bond, f_1, is

$$f_N = Nf_1$$

since each bond is subjected to $1/N$ of the total force. A better model of the rupture of a single bond is that it is a thermally activated process and stochastic in nature. There is no definite bond rupture force, but rather a force-biased rate for rupture that is described well by the Bell model and subsequent refinements by Evans and others.[34-37] In the Bell model[38] the lifetime of a bond under an applied tensile force is:

$$f = \frac{k_B T}{\chi_\beta} \ln\left(\frac{r\chi_\beta}{k_{off} k_B T}\right)$$

where χ_β is the effective width of the bond potential, r is the rate at which the bond is loaded, and k_{off} is the equilibrium disassociation constant.

When the load is distributed across multiple bonds, the theory must be generalized to account for the collective behavior of the bonds under load. Different theories have been proposed based on assumptions about the collective behavior of the bonds during the rupture process.

A theory due to Tees et al.[33] again assumes that the bonds are identical and loaded equally, but that each individual bond ruptures at a rate given by the Bell model.[38] Using a form of Bayesian statistics known as reliability theory and various loading curves, they calculated the average force to rupture all of the bonds scales approximately with the Harmonic number[33], $H_N = \Sigma(1/k)$; i.e. 1,1.5,1.87,... for 1,2,3,... bonds:

$$f_N \cong H_N f_1$$

This kind of rupture process in which all bonds are equal is analogous to the process of spallation in the fracture mechanics of solids, where due to the rapidity of dynamic fracture, different regions of the material fracture independently.[39] In more conventional cracking, the crack has a definite tip, and the bonds at the tip are loaded more than the others. In multivalent bond rupture, similar considerations apply to the Zipper model proposed by Williams.[34] Based on the stochastic single-bond rupture theory of Evans and Ritchie,[37] this model predicts that the mean rupture force increases logarithmically with the multiplicity of the binding:

$$f_Z = f_1 + f_\beta \ln(N)$$

where f_Z is the force required to rupture the zipper, f_1 equals the single-bond rupture force, f_β is the force scaling factor (~40 pN for our system), and N is the number of connections.

Interestingly enough, our results for multivalent forces (66 and 85 pN) agree equally well with both models. Reliability theory produces values for multivalent rupture of 70.5 pN for two bonds and 86.2 pN for three bonds, assuming a single bond rupture force of 46 pN. The zipper model gives ~74 pN and 90 pN for two and three bonds, assuming a 46 pN single-bond rupture force and a force scaling factor (f_β) of 40 pN. Note that in both the model of Tees et al. and the model of Williams that the force scaling with the number of bonds is nonlinear. In both cases it is sub-linear, so that doubling the number of bonds less than doubles the rupture force, as we observe in the experiments. While neither of these models has been tested extensively, both make definite predictions about multivalent bond rupture and it is interesting to compare the results of our measurements with those predictions. In any case, we offer

these analytical treatments simply to provide theoretical evidence for nonlinearly additive force behavior for multiple connections. Certainly additional studies must be done in order to validate these or other models of multivalent force behavior.

Polymer Architecture, Single Versus Multiple Proteins As previously mentioned there have been several force experiments measuring *multiple* proteins on one surface binding to multiple ligands on another surface. The case of a *single* protein binding to multiple ligands is quite different in nature, and of great interest because of the potential for cooperativity in binding and the resulting implications for function. It is important then for the analysis to assess whether the candidate multivalent binding events involve only a single protein and therefore represent multivalency in its most fundamental form. Because the interactions that we include in our analysis are more than a single polymer tether length (>~30 nm) from the point of tip-substrate contact, we can be reasonably certain that both the ConA tetrameric protein and the mannose ligands are on tethers. The tethering leads to three possible configurations for the interactions between the tip and the substrate as shown in Fig. 5, consisting of two, three (or more), and four polymers binding, which we denote as I, λ and II, respectively, to indicate the envisaged configuration. To be specific, the λ configuration consists of one polymer bound to two or more polymers. The II configuration would essentially mean that the AFM tips that we were using for our experiments were functionalized with multiple active proteins rather than just one as we discuss in the introduction and materials and methods. As we discard tips that display multiple interactions at greater than single tether lengths with frequencies higher than 0.5% of the total interactions, it is unlikely that the tips used for these measurements bear more than one functional tethered protein. Two polymers binding (I) multivalently would imply that the substrate sometimes contains multiple mannose ligands bound to a single polymer tether. This configuration is also unlikely, as the α-D-mannopyranosylphenyl ligand only contains a single isothiocyanate group that is used to link the ligand to the polymer[40] limiting the possibility that the mannose ligands form polysaccharide-like structures. We believe that the λ configuration is the most probable although we cannot completely rule out the possibility of the other configurations. To clarify this issue we performed calculations to determine how

stretching three and four polymers linked in a λ configuration would differ from the other two cases. These calculations were then used to fit the data.

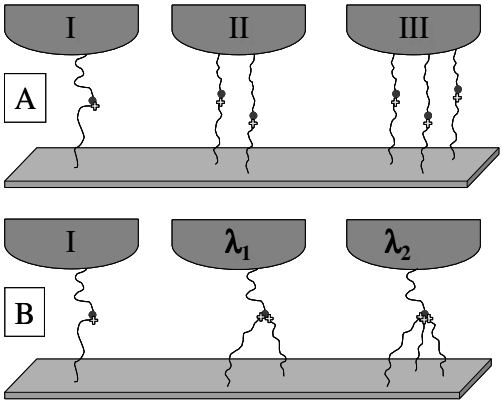

Figure 3. A cartoon (not to scale) of possible configurations for the interactions between proteins (black circles) tethered to the cantilever tip and ligands (open crosses) tethered to the substrate. In scenario A each protein interacts with a single ligand resulting in essentially parallel connections between the tip and the substrate. In scenario B a single tethered protein interacts with multiple tethered ligands, leading to a branched polymer architecture connecting the tip and substrate. For identical polymers these configurations show distinct differences in their stretching profiles, as described by formulas given in the text. Note that in reality there may be many additional polymers on the substrate and on the tip, only a fraction of which participate in the interactions between the tip and the substrate due to physical or chemical constraints that prevent the formation of specific bonds.

The principal query is to assess whether the polymer stretching signatures seen in our data are consistent with the λ configuration of WLC tethers. This force law is not described in the existing literature to the best of our knowledge. We derive it in detail elsewhere,[41] and only present it here with a brief motivation. In addition, we have derived the analogous formulas for the freely-jointed chain (FJC) model, which is also used to model polymer extension. Here we also compare the polymer stretches to the WLC force laws for the I and II configurations.

The formula for force as a function of extension for the I configuration is well known,[23] with the minor extension that the force law for two WLC's attached end to end is the same as the force law for a single WLC whose contour length is the sum of that of the two WLC's. The I-configuration WLC force, f_I, as a function of extension, z, is given by

$$f_I = \frac{k_B T}{l_p}\left[\frac{1}{4(1-z/l_{tot})^2} - \frac{1}{4} + \frac{z}{l_{tot}}\right],$$

where k_B is the Boltzmann constant, T is the absolute temperature, l_p is the PEG persistence length and l_{tot} is the sum of the contour lengths of the two PEG's. This expression and the ones that follow assume that the size of the functional groups is small compared to the PEG contour lengths.

The force law for the II configuration is simply twice the force for the I configuration since forces add for springs in parallel, even for non-linear WLC springs. More generally, the force for n identical WLC's in parallel is n times the force for a single WLC with the same extension. The II-configuration WLC force, f_{II}, as a function of extension, z, is given by

$$f_{II} = \frac{2k_B T}{l_p}\left[\frac{1}{4(1-z/l_{tot})^2} - \frac{1}{4} + \frac{z}{l_{tot}}\right]$$

where for n PEG's in parallel the leading 2 would be replaced by n.

Finally, the force law for the λ configuration is more complicated to derive since it results from solving the equation of equilibrium for a single WLC and a pair of WLC's. Since the force law for each WLC is non-linear, an exact analytic expression for the force is only possible in certain limits. Nevertheless, the force can be calculated to arbitrary precision numerically and we have used the numerical solution to find an approximate analytic form that is good to better than 4% everywhere, a level of accuracy more than sufficient for our purposes here. The approximate analytic form is

$$f_\lambda \cong \frac{k_B T}{l_p}\left\{\alpha\left[\frac{1}{4(1-z/l_{tot})^2} - \frac{1}{4}\right] + \beta\frac{z}{l_{tot}}\right\}$$

$$\alpha = \left(\frac{l_0 + \sqrt{n}l_0'}{l_0 + l_0'}\right)^2 = 1.457(n=2), 1.866(n=3)$$

$$\beta = \frac{3}{2}\left(\frac{l_0 + l_0'}{l_0 + l_0'/n}\right) - \frac{1}{2}\alpha = 1.271(n=2), 1.317(n=3)$$

where α and β are given by the forms in the second line when the single tip-linked tether has contour length l_0 and the n substrate-linked tethers have contour length l_0'. The numerical values given for α and β apply when all tethers have the same contour length l_0. Taking the measured variation in the PEG length distribution into account, α and β can vary by +/-2% (assuming that the PEG attaching the protein is the same throughout the measurements).

We have fit the λ-configuration (with n = 2, and n = 3) and II-configuration generalized WLC force laws to the experimental force-extension data for the candidate multivalent binding events. For these fits T = 300K and the persistence length l_p was held at 3.5Å as reported from experiment.[42,43] The zero force point was allowed to vary across the range ±15 pN, a conservative estimate for the error in the system, while the polymer contour length, l_p, was allowed to vary from 38-50 nm, the approximate contour length for our polymer tethers. Typical fits are shown in Fig. 6 where the λ-configuration is clearly superior to the II-configuration. The λ-configuration fits shown are for n = 2, the difference in the quality of the fit between n = 2 and n = 3 is ~2 pN, well within the average error value for all fits. In all we have fit an additional 10 candidate multivalent curves (Fig. 6) with average error values of 2.6 ± 0.17 pN for the λ-configuration and 13.2 ± 4.8 pN for the II-configuration. The ability to fit the data well with the λ-configuration force law adds support to the hypothesis that two mannose-functionalized PEG's are bound to a single ConA-functionalized PEG. This conclusion raises an interesting question: if we are indeed measuring the unbinding of two (or more) mannose-functionalized polymers from a single protein-functionalized polymer, why do we typically see only a single specific unbinding event in our force curves rather than multiple unbinding events? Certainly, assuming a λ-configuration with two identical length polymers bound to the protein through two identically strong protein-ligand bonds, we would expect that both bonds would rupture simultaneously. This immediacy follows from the fact that once the first bond is ruptured, the force on the second bond will increase from a value that was already sufficient to rupture the identical first bond.

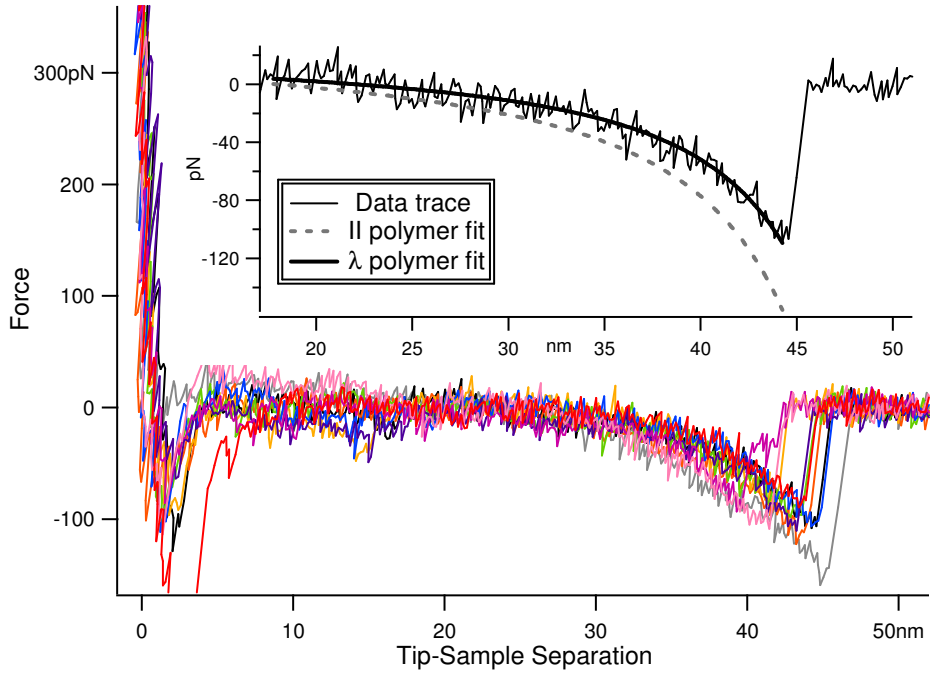

Figure 4. Ten experimental force-distance curves (from the data plotted in the inset of Fig. 2) showing the characteristic polymer stretching and bond rupture between 40 and 55 nm from the point of tip-sample contact. The inset shows fits of the generalized WLC model for the λ-configuration (n=2, average error = ~1.5 pN) and II-configuration (average error = ~14.4 pN) to polymer stretching data from a single experimental force curve. For these fits the zero force point was allowed to vary from -15-15 pN, a conservative estimate for the error in the system, while the polymer contour length, l_p, was allowed to vary from 40-50 nm, the approximate contour length for our polymer tethers. In all fits the λ-configuration (average error = 2.6 ± 0.17 pN) was clearly better than the II-polymer configuration (average error= 13.2 ± 4.8 pN). Due to the noise in our force traces we were unable to differentiate between fits to λ (n=2) and λ (n=3.)

In the opposite case, if the second bond is much stronger than the first bond, or if the second PEG is much longer than the first PEG, the second bond will not rupture until a much greater extension, and the second rupture will be clearly distinguished from the first.

The real situation is between these two extremes, and it depends on the PEG configuration. Generally, the λ configuration can be expected to exhibit a single rupture, whereas the II configuration exhibits two.

To see why, first consider what would happen if the PEG's were linear springs attached to a rigid cantilever. In the λ configuration, when the first bond ruptures, a force imbalance arises, and the connection at the ConA moves in the direction of the initially unpaired PEG. The unpaired PEG extension relaxes from 2/3 to 1/2 of the span from the tip to the substrate. In the process the force on the remaining bond rises by 50%. Taking into account the cantilever spring back and the non-linearity of the WLC force law, this increase can be well over 100% (the full analysis is not presented here) and the two ruptures appear as a single event in the force curve even when the second PEG is up to 10nm longer (the maximum possible length difference for our tethers as measured by mass spectrometry, see experimental, substrate functionalization.) In the II configuration, the situation is different. Again consider linear springs and a rigid cantilever first. When the first bond breaks, the load on the second bond would remain unchanged since the PEG's extension would not change. If the cantilever is allowed to spring back, the force on the second bond would rise slightly, by a fraction equal to the ratio of the PEG and cantilever spring constants. Since the cantilever is much stiffer than the PEG, its force drops precipitously in a spring back of only a few nanometers, whereas the PEG force only rises slightly. These basic mechanics continue to hold for the non-linear WLC force laws associated with real PEG's (the detailed analysis is not presented here), and the two bond ruptures would typically appear as separate events in the force curve. The observation of only single rupture events in the force curve gives additional evidence for the λ configuration.

We have considered how well the force-extension curve could be fit with a generalized WLC force law suitable for the I, λ, and II configurations. In most cases we find that while the λ-configuration force law provides the best fit, the I configuration cannot be ruled out due to the noise in the force traces. As the II configuration cannot be used to fit the data we can be confident that regardless of whether the protein is somehow interacting serially with two ligands on a single tether- as in the I configuration- or more plausibly interacting with two or more ligands on separate tethers- as in the λ configuration- we are indeed measuring the single protein- multiple ligand rupture force. In addition, although the generalized

WLC forces are not sufficient by themselves to differentiate between the I and λ configurations, the probability of the I molecular architecture is lessened by consideration of the chemistry.

Multiple peaks in Tip-Sample Separation Histograms When the protein was dimeric the final cluster contained a single peak in the tip-sample separation distance histogram (Fig. 1A.) Surprisingly with a tetrameric protein the final interaction cluster displayed two peaks roughly 4 nm apart (Fig. 1C.) This double peak was unexpected as it indicated that the adhesive interactions were occurring at more than one tip-sample separation distance. Multiple peaks in the tip-sample separation distance histogram often indicate that the AFM tip being used to make the measurement has been functionalized with multiple polymer-tethered proteins and thus it was a matter for concern. However, as previously discussed, we decrease the possibility of multiply-functionalized tips by discarding all tips that display multiple specific bond ruptures at greater than a single tether length from the substrate. In addition, fitting the force curves with modified WLC models indicated that the polymers linking the tip to the substrate were stretching in the branched or λ configuration, lending credence to the idea that the tips we use have only a single polymer-tethered protein that can actively bind ligands.

In our previous work we showed that peaks in the tip-sample separation histograms indicate that adhesive interactions are occurring at a distance that is equal to the length of the polymer on the tip plus the length of the polymer on the substrate. Because the tethered protein on the tip can link to any polymer on the substrate, the width of the specific interaction cluster is defined by the polydispersity in length of the polymers on the substrate, about 10 nm.[1] The dimeric form and the tetrameric form only differ in cross-section by around 1 nm, meaning that the additional length of the tetrameric protein could not be responsible for the double peak. Gently rinsing the tip with buffer at pH 6.0 to remove the aggregated protein and leave just the dimer, and then repeating the experiment at pH 7.4, resulted in the abolishment of the second peak. This result indicates that the tetrameric form of the protein was responsible for the double peak, and that the second peak was not a direct consequence of the higher pH. Similarly, adding unbound ligand to the buffer solution decreased the frequency of the final cluster to

background levels, indicating that the cluster was indeed due to the specific ConA-mannose interaction (Fig. 1D).

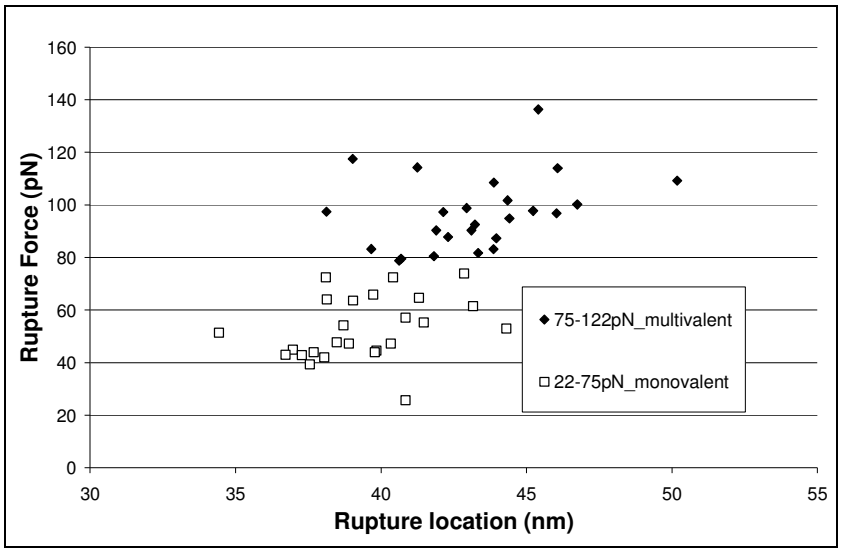

Figure 5. Rupture force vs. rupture location data taken with a single AFM cantilever divided into two force ranges, a lower force range that included all interactions measured between 22 and 75 pN, and a higher range of forces measured between 75 and 122 pN. The graph clearly indicates a correlation between the force and the location at which the bond rupture occurred. These points represent the data plotted in the inset to Fig. 2.

We reasoned that variances in tip functionalization could cause the location of the specific bond cluster to vary, however if there is only a single polymer-tethered protein on the cantilever, then the specific interaction cluster in the tip-sample histogram should contain only a single peak. We therefore divided the interactions into two force sets and graphed the rupture force as a function of the rupture location (Fig. 5). This plot revealed that the weaker rupture forces tended to occur at lesser tip-sample separation distances (~40 nm) in comparison to the stronger rupture forces (~44 nm) (see Fig. 6.) We hypothesized that if we were indeed measuring multiple rupture forces due to monovalent and multivalent interactions, the multivalent and therefore stronger bonds were stretching the polymer tethers an additional distance prior to rupture.

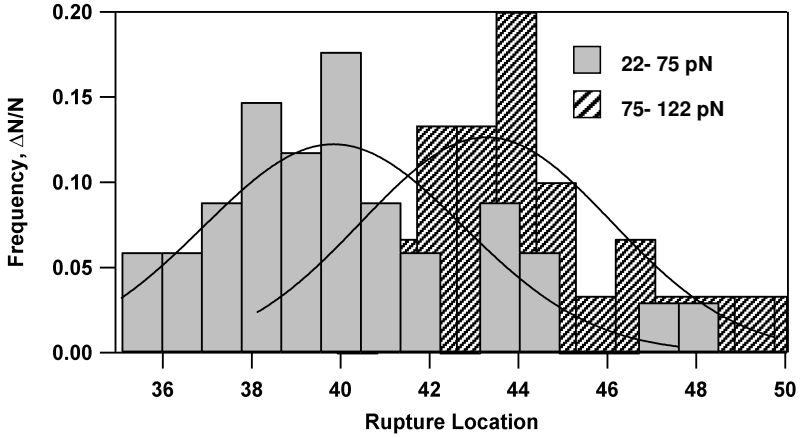

Figure 6. Histograms of the frequency of interactions vs. rupture location for the force separated data shown in Fig. 5. Note that the centers of the distributions are separated by ~4 nm. This distance roughly corresponds to the additional polymer extensions due to the approximately 30 pN average difference between the monovalent and the multivalent interactions.

To test this hypothesis, we used our WLC models to simulate force spectroscopy data and evaluate whether the higher forces that we measured were correlated with the increased distances (not shown). Not surprisingly, for a 50 nm polymer chain (the average effective length of our linked protein and ligand) the application of an additional ~30 pN of force corresponds to an additional ~4 nm stretch. The additional stretching increased the width of the specific tetrameric ConA-mannose cluster in the tip-sample distance histogram relative to the dimeric form of the protein, and had the added effect of generating two peaks in the rupture location histogram. Multiple peaks in the tip-sample separation histogram are therefore indicative of multiple force distributions and thus multivalent interactions.

CONCLUSIONS

We have continued our research into protein-carbohydrate adhesion by measuring the forces required to rupture multiple carbohydrate linkages to a protein. We find that the rupture forces do not scale linearly additively, as described previously. The divalent and trivalent rupture forces are significantly less than twice and three times the monovalent rupture force and are consistent with two theoretical treatments for multivalent bond rupture behavior. Similarly to our previous work we use polymer tethers to attach the protein to the tip and the carbohydrates to the substrate. Previously we found that

tethering the binding partners produced accurate data where the specific binding forces between the protein and receptor could be separated from nonspecific adhesion between the tip and substrate and between the protein and the substrate. Here we have shown that fitting the force-extension curves with a generalized WLC model allows a determination of serial (one protein bound to multiple ligands) versus parallel (multiple proteins bound to multiple ligands) connections between the tip and substrate. To our knowledge, this is the first study that permits an unambiguous measurement of the multivalent adhesive forces between a single protein and carbohydrates.

ACKNOWLEDGMENT: We would like to thank Christine Orme, Raymond Friddle, and Todd Sulchek for useful discussions and gratefully acknowledge funding by the LLNL Laboratory Directed Research and Development program. This work was performed under the auspices of the US Dept. of Energy by the Univ. of California/Lawrence Livermore National Laboratory under Contract No. W-7405-Eng-48.

REFERENCES

(1) Ratto, T. V.; Langry, K. C.; Rudd, R. E.; Balhorn, R. L.; Allen, M. J.; McElfresh, M. W. *Biophys J* **2004**, *86*, 2430-2437.
(2) Varki, A. *Glycobiology* **1993**, *3*, 97-130.
(3) Yarema, K. J.; Goon, S.; Bertozzi, C. R. *Nat Biotechnol* **2001**, *19*, 553-558.
(4) Lis, H.; Sharon, N. *Chemical Reviews* **1998**, *98*, 637-674.
(5) Hauri, H. P.; Appenzeller, C.; Kuhn, F.; Nufer, O. *FEBS Letters* **2000**, *476*, 32-37.
(6) Gut, A.; Kappeler, F.; Hyka, N.; Balda, M. S.; Hauri, H. P.; Matter, K. *EMBO Journal* **1998**, *17*, 1919-1929.
(7) Kiessling, L. L.; Pohl, N. L. *Chemistry & Biology* **1996**, *3*, 71-77.
(8) Lee, Y. C.; Lee, R. T. *Accounts of Chemical Research* **1995**, *28*, 321-327.
(9) Wong, C. H. *Accounts of Chemical Research* **1999**, *32*, 376-385.
(10) Kiessling, L. L.; Cairo, C. W. *Nat Biotechnol* **2002**, *20*, 234-235.
(11) Kiessling, L. L.; Gestwicki, J. E.; Strong, L. E. *Current Opinion in Chemical Biology* **2000**, *4*, 696-703.
(12) Bertozzi, C. R.; Kiessling, L. L. *Science* **2001**, *291*, 2357-2364.
(13) Dam, T. K.; Brewer, C. F. *Chemical Reviews* **2002**, *102*, 387-429.
(14) Dimick, S. M.; Powell, S. C.; McMahon, S. A.; Moothoo, D. N.; Naismith, J. H.; Toone, E. J. *Journal of the American Chemical Society* **1999**, *121*, 10286-10296.
(15) Marshall, B. T.; Long, M.; Piper, J. W.; Yago, T.; McEver, R. P.; Zhu, C. *Nature* **2003**, *423*, 190-193.
(16) Merkel, R. *Physics Reports-Review Section of Physics Letters* **2001**, *346*, 344-385.
(17) Chen, A. L.; Moy, V. T. *Atomic Force Microscopy in Cell Biology* **2002**, *68*, 301-309.
(18) Florin, E. L.; Moy, V. T.; Gaub, H. E. *Science* **1994**, *264*, 415-417.

(19) Lee, G. U.; Kidwell, D. A.; Colton, R. J. *Langmuir* **1994**, *10*, 354-357.
(20) Raab, A.; Han, W. H.; Badt, D.; Smith-Gill, S. J.; Lindsay, S. M.; Schindler, H.; Hinterdorfer, P. *Nat Biotechnol* **1999**, *17*, 902-905.
(21) Riener, C. K.; Stroh, C. M.; Ebner, A.; Klampfl, C.; Gall, A. A.; Romanin, C.; Lyubchenko, Y. L.; Hinterdorfer, P.; Gruber, H. J. *Anal Chim Acta* **2003**, *479*, 59-75.
(22) Evans, E.; Ritchie, K. *Biophys J* **1999**, *76*, 2439-2447.
(23) Marko, J. F.; Siggia, E. D. *Macromolecules* **1995**, *28*, 8759-8770.
(24) Oberdorfer, Y.; Fuchs, H.; Janshoff, A. *Langmuir* **2000**, *16*, 9955-9958.
(25) Oberdorfer, Y.; Schrot, S.; Fuchs, H.; Galinski, E.; Janshoff, A. *Phys Chem Chem Phys* **2003**, *5*, 1876-1881.
(26) Grandbois, M.; Beyer, M.; Rief, M.; Clausen-Schaumann, H.; Gaub, H. E. *Science* **1999**, *283*, 1727-1730.
(27) Butt, H. J.; Jaschke, M. *Nanotechnology* **1995**, *6*, 1-7.
(28) Florin, E. L.; Rief, M.; Lehmann, H.; Ludwig, M.; Dornmair, C.; Moy, V. T.; Gaub, H. E. *Biosensors & Bioelectronics* **1995**, *10*, 895-901.
(29) Hutter, J. L.; Bechhoefer, J. *Rev Sci Instrum* **1993**, *64*, 3342.
(30) Jaschke, M.; Butt, H. J. *Rev Sci Instrum* **1995**, *66*, 1258-1259.
(31) Baker, G. A. *Essentials of Padâe approximants*; Academic Press: New York,, 1975.
(32) Seifert, U. *Phys Rev Lett* **2000**, *84*, 2750-2753.
(33) Tees, D. F. J.; Woodward, J. T.; Hammer, D. A. *J Chem Phys* **2001**, *114*, 7483-7496.
(34) Williams, P. M. *Anal Chim Acta* **2003**, *479*, 107-115.
(35) Hummer, G.; Szabo, A. *Abstr Pap Am Chem S* **2004**, *227*, U897-U897.
(36) Gopich, I.; Hummer, G.; Szabo, A. *Abstr Pap Am Chem S* **2003**, *226*, U287-U287.
(37) Evans, E.; Ritchie, K. *Biophys J* **1997**, *72*, 1541-1555.
(38) Bell, G. I. In *Science*, 1978; Vol. 200, pp 618-627.
(39) Meyers, M. A. *Dynamic behavior of materials*; Wiley: New York, 1994.
(40) Sigma-Aldrich *private communication*.
(41) Rudd, R. E.; Ratto, T. V. *manuscript in preparation*
(42) Kenworthy, A. K.; Simon, S. A.; Mcintosh, T. J. *Biophys J* **1995**, *68*, 1903-1920.
(43) Rex, S.; Zuckermann, M. J.; Lafleur, M.; Silvius, J. R. *Biophys J* **1998**, *75*, 2900-2914.